Mathematical Model on the Sensing Behavior of a Biooxidation Biosensor

Y. Chen and T. C. Tan
Dept. of Chemical Engineering, National University of Singapore, 10 Kent Ridge Crescent, Singapore 0511

A phenomenological model developed describes the steady-state sensing characteristics of a biosensor based on biooxidation of organic solutes by dissolved oxygen. The model is experimentally verified using a recently developed dopamine sensor that enzymatically oxidizes dopamine by polyphenolase in apple tissues. It adequately describes its steady-state sensing characteristics, including the effects of mass of immobilized apple fines in the biofilm, temperature, and pH of the substrate solution. The parameters provide a basis for evaluating the suitability of different bioactive materials or the same bioactive material from different sources for biosensor fabrication. At zero thickness of the membranes and biofilm, the model describes the sensing characteristics of a dissolved oxygen probe in which the oxygen diffusivity through the Teflon membrane is 9.83×10^{-11} m^2/s, *comparable with a previously reported value. It can also describe the sensing behavior of any nonbiocatalyzed oxidation-related sensor in a two-substrate system simply by replacing the governing faradaic equations for the dissolved oxygen probe with those appropriate to the type of probe used.*

Introduction

A sensor is used to measure the solute concentration of a solution by monitoring a concentration-dependent property of the solution. In the absence of such an appropriate concentration-dependent property, the solute may be chemically converted and its concentration is indirectly measured by monitoring the concentration of one of its reaction products or its coreactant using an appropriate probe. Catalytic gas sensors and biosensors are operated on this principle. A biosensor therefore consists of (1) a biofilm in which a bioactive material is immobilized to effect a biochemical reaction and (2) a probe to measure the concentration of a reaction product or coreactant. For a biooxidation reaction, a dissolved oxygen probe is normally used to monitor the oxygen concentration (Figure 1). Many biosensors have been developed for monitoring the concentration of organic solutes in aqueous solutions. These include enzymatic sensors for the quantitative sensing of glucose, alcohol, and cholestrol (Clark, 1987), microbial sensors for process and environmental monitoring such as the biochemical oxygen demand of organic trade effluents and wastewater (Karube, 1986, 1987; Riedel et al., 1989; Tan et al., 1992), and tissue sensors for the monitoring of tyrosine, ascorbic acid, and dopamine (Arnold and Rechnitz, 1987; Sidwell and Rechnitz, 1986; Tan and Chen, 1993). Biosensors are increasingly being used for routine chemical analysis and clinical diagnosis (Albery and Craston, 1987; Clark, 1987; Karube, 1987; Rechnitz, 1975, 1981).

The sensing characteristics of a biosensor depend significantly on the various rate processes occurring in the system, such as diffusion, adsorption of reactive solute on the biocatalyst structure, reaction kinetics, and faradaic reactions at the surface of the sensing electrode. There has been sustained interest in mathematical modeling on relating the sensor response to these various rate processes. Earlier, biosensors were developed mainly for monitoring the concentration of a single solute in a solution or a one-substrate solution. Various mathematical models have been proposed for such systems. The models proposed by Blaedel et al. (1972) and Mell and Maloy (1975) for enzymatic sensors were verified within experimental constraints. Response characteristics were simulated by Mell and Maloy (1975) for both enzymatic reaction and diffusion-controlled regimes. Through an orthogonal collocation technique, Brady and Carr (1980) were able to simulate the steady-state response characteristics of a similar biosensor. Jochum and Kowalsk (1982) mathematically analyzed the effect of stirring on the transient and pseudo-steady-state behaviors of biosensors with potentiometric or amperometric sensing electrodes. Eddowes (1990) and Hameka and Rechnitz (1983) described the system with re-

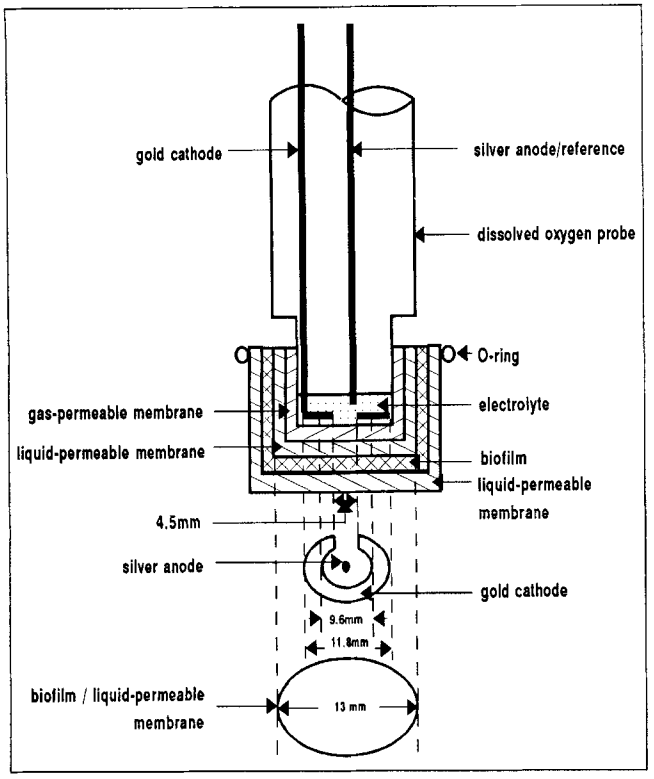

Figure 1. Typical configuration of a biosensor.

spect to the concentration profile of the substrate in the system. Mathematical analysis (Lemke, 1988b) was also extended to include biosensors containing functional membranes that helped improve their selectivity and stability.

Most biocatalyzed reactions involve more than one reactant or substrate in the solution, and biosensors are sometimes classified by the number of substrates involved. Biocatalyzed oxidation is the most common two-substrate (oxygen and the organic solute) system. A dissolved oxygen probe is usually used in these two-substrate biooxidation sensors to relate the oxygen concentration to the substrate concentration in the solution. Mathematical analysis of the sensing characteristics of dissolved oxygen probes has been carried out by Jensen et al. (1978), Gough and Leypoldt (1980), Hale and Hitchman (1980), Firouztale et al. (1982), Myland and Oldham (1984), Vacek et al. (1986), and Lemke (1988a). Leypoldt and Gough (1984) simplified their steady-state analysis of a two-substrate biosensor to a single membrane (biofilm) system by assuming negligible mass-transfer resistance in the dissolved oxygen probe compared with that in the biofilm. This was extended by Gough et al. (1985) to a two-dimensional description of enzymatic glucose sensors. Tatsuma and Watanabe (1992) also extended their steady-state, single-membrane model to include an additional functional membrane besides the biofilm.

This article describes a steady-state phenomenological model for a two-substrate biosensor based on the biocatalyzed oxidation of the sensed organic solute by a bioactive material immobilized in the biofilm. The model relates the sensor response to the rate phenomena occurring during the sensing process. The model was verified using experimental data obtained with an apple tissue dopamine sensor at different temperatures, pHs, and amounts of immobilized apple fines in the biofilm.

Development of the Model

Sensor configuration

Figure 1 shows the general construction of a biooxidation biosensor. The biofilm is prepared by immobilizing a bioactive material, such as a microorganism (microbial sensor), purified enzyme (enzymatic sensor), whole cell, or tissue (tissue sensors), on top of a liquid-permeable membrane using a suitable polymeric solution. The biofilm, with its supporting membrane, is placed on top of the gas-permeable membrane of a dissolved oxygen probe with the immobilized bioactive material on the outside. Another liquid-permeable membrane is placed over the biofilm to prevent any bioactive material dislodged during the operation from contaminating the substrate solution. The combined membrane/biofilm/membrane is stretched tightly over the gas-permeable membrane of the oxygen probe and secured properly with a tightly fitting rubber O-ring.

Steady-state measurement procedure

Steady-state measurement with a biooxidation biosensor involves measuring the steady-state current response in an air-saturated buffer solution before (I_o) and after the addition of the organic solute (I_s). The concentration of the organic solute in the sample solution is then obtained from a calibration curve relating the sensor response, ($I_o - I_s$), to the organic solute concentration. The development of the mathematical model therefore involves relating the sensor response to the various rate processes occurring in the sensing process.

Rate phenomena and sensing behavior

When a biooxidation biosensor is placed in an air-saturated buffer solution, oxygen from the buffer solution diffuses through the various membranes and phases toward the dissolved oxygen electrodes. Figure 2a shows typical steady-state oxygen concentration profiles established in the sensor according to the diffusional resistance of each phase, namely the air-saturated buffer solution (0), the outer liquid-permeable membrane (I), the biofilm (II), the inner liquid-permeable membrane (III), the gas-permeable membrane (IV), and the electrolyte (V) of the dissolved oxygen probe. The buffer is usually well-agitated mechanically and by the continuous flow of air through the solution such that the conditions at its interface with the liquid-permeable membrane (I) are the same as in the bulk solution. At the interface between the inner liquid-permeable membrane (III) and the gas-permeable membrane (IV), only oxygen diffuses through the gas-permeable membrane and is absorbed into the electrolyte (V) of the dissolved oxygen probe. At both the interfaces with the gas-permeable membrane, the partial pressure of the oxygen gas in the gas-permeable membrane would be at equilibrium with the dissolved oxygen in the liquid-permeable membrane and in the electrolyte, respectively. When the organic substrate is introduced into the buffer, the organic solute diffuses through the outer liquid-permeable membrane (I) and

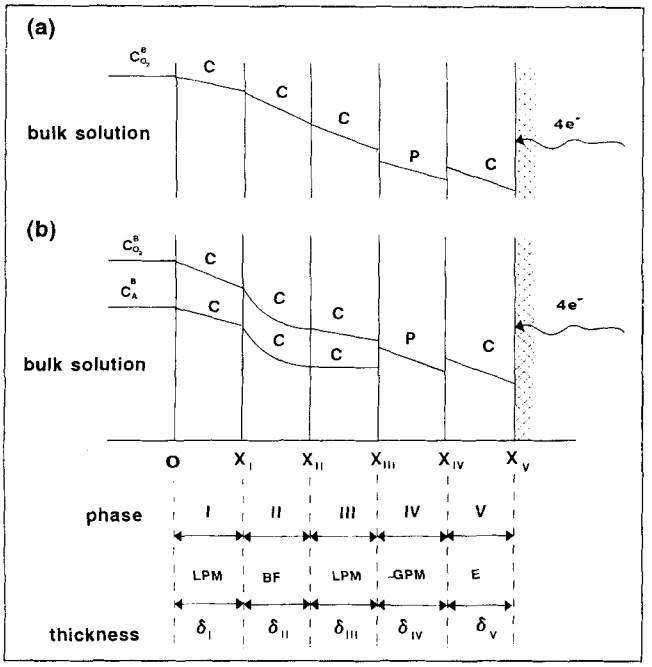

Figure 2. Concentration profiles of oxygen and dopamine in the various phases.

(LPM = liquid-permeable membrane; BF = biofilm; GPM = gas-permeable membrane; E = electrolyte.)

into the biofilm (II) where it is catalytically oxidized by the bioactive material during its diffusion toward the inner liquid-permeable membrane (III). At the interface with the gas-permeable membrane (IV), the organic solute is blocked from entering the gas-permeable membrane. The oxygen, however, continues to diffuse through the gas-permeable membrane to be absorbed into the electrolyte V of the dissolved oxygen probe. Similar gas/liquid equilibrium for oxygen can be assumed to prevail at the two interfaces with the gas-permeable membrane. Figure 2b shows the steady-state concentration profiles of the two substrates. The amount of oxygen consumed during the biooxidation of the organic solute in the biofilm depends on the concentration of the organic solute, the rates of diffusion, and the kinetics of the biooxidation reaction.

Mathematical model

The approach to the problem is to establish the phenomenological relationships of the concentration profiles of the two substrates and to relate the oxygen concentration to the current response of the dissolved oxygen probe. The functional relationship for the difference in the current responses obtained with and without the presence of the organic solute is then derived in terms of the phenomenological parameters and the concentration of the organic solute.

Buffer Solution Containing No Biooxidizable Organics. Normally an air-saturated buffer solution is used as the inert carrier to maintain the desired optimum pH for the biooxidation reaction in the biofilm. Under steady-state conditions, the general mass balance equation for oxygen across each membrane, biofilm, and electrolyte shown in Figure 2a is given by

$$D^J_{O_2}\frac{d^2C^J_{O_2}}{dx^2} = 0 \tag{1}$$

where $D^J_{O_2}$ is the effective diffusivity of dissolved oxygen in phase J. The general solution to Eq. 1 is given by

$$C^J_{O_2} = a^J_o x + a^J_1 \tag{2}$$

where a^J_o is the oxygen concentration gradient in phase J, which is constant at a given temperature. The general boundary conditions, except for $x = 0$ (substrate solution/liquid-permeable membrane I interface) and $x = x_V$ (cathodic surface of the dissolved oxygen probe), are:

$$x = x_J, \qquad C^J_{O_2} = C^{J+1}_{O_2} \tag{3}$$

$$x = x_J, \qquad D^J_{O_2}a^J_o = D^{J+1}_{O_2}a^{J+1}_o. \tag{4}$$

With vigorous stirring of the substrate solution, the oxygen concentration at $x = 0$ can be assumed to be the same as the bulk concentration, $C^B_{O_2}$. The same assumption was used by Jochum and Kowalski (1982) and Tatsuma and Watanabe (1992). The dissolved oxygen probe is normally designed to operate under limiting current conditions, which implies that at $x = x_V$, $C^V_{O_2} = 0$. The oxygen concentration profile for each of the phases can therefore be determined as shown in the following equations:

Liquid-Permeable Membrane (I) with Thickness = δ_I.

$$C^{I}_{O_2} = a^{I}_o x + C^B_{O_2}. \tag{5}$$

Biofilm (II) with Thickness = δ_{II}.

$$C^{II}_{O_2} = a^{II}_o(x - \delta_I) + a^{I}_o\delta_I + C^B_{O_2}. \tag{6}$$

Liquid-Permeable Membrane (III) with Thickness = δ_{III}.

$$C^{III}_{O_2} = a^{III}_o(x - \delta_I - \delta_{II}) + a^{II}_o\delta_{II} + a^{I}_o\delta_I + C^B_{O_2}. \tag{7}$$

Gas-Permeable Membrane (IV) with Thickness = δ_{IV}. At the interface between the liquid-permeable membrane (III) and the gas-permeable membrane (IV), the equilibrium conditions are described by Henry's law, since the oxygen concentration is small.

$$P_{O_2} = H_{O_2}[C_{O_2}]. \tag{8}$$

The concentration profile in terms of partial pressure of oxygen is then given by

$$P^{IV}_{O_2} = H_{O_2}\left[a^{IV}_o(x - \delta_{III} - \delta_{II} - \delta_I) + a^{III}_o\delta_{III} + a^{II}_o\delta_{II} + a^{I}_o\delta_I + C^B_{O_2}\right]. \tag{9}$$

Electrolyte (V) with Thickness = δ_V. Similar gas-liquid phase equilibrium can be assumed at the interface between the gas-permeable membrane (IV) and the electrolyte (V) of the dissolved oxygen probe. The concentration profile is therefore given by

$$C^{V}_{O_2} = a^{V}_{o}(x - \delta_{IV} - \delta_{III} - \delta_{II} - \delta_{I}) + a^{IV}_{o}\delta_{IV} + a^{III}_{o}\delta_{III} + a^{II}_{o}\delta_{II} + a^{I}_{o}\delta_{I} + C^{B}_{O_2}. \quad (10)$$

The boundary conditions provide the link among the various concentration gradients of the different phases as shown in Eq. 11.

$$D^{I}_{O_2}a^{I}_{o} = D^{II}_{O_2}a^{II}_{o} = D^{III}_{O_2}a^{III}_{o} = D^{IV}_{O_2}a^{IV}_{o} = D^{V}_{O_2}a^{V}_{o}. \quad (11)$$

Since at $x = x_V$, the oxygen concentration is zero, the concentration gradient in the liquid-permeable membrane (I) is given by solving Eqs. 10 and 11.

$$a^{I}_{o} = \left[\frac{-C^{B}_{O_2}}{\varphi_{O(I/V)}\delta_{V} + \varphi_{O(I/IV)}\delta_{IV} + \varphi_{O(I/III)}\delta_{III} + \varphi_{O(I/II)}\delta_{II} + \delta_{I}}\right] \quad (12)$$

where the diffusivity ratio $\varphi_{s(J/K)}$ is defined as

$$\varphi_{s(J/K)} = \frac{D^{J}_{s}}{D^{K}_{s}} \quad (13)$$

in which s is the substrate solute (o for oxygen and A for biooxidizable solute); J and K are the adjacent phases.

Calibration Constant of Dissolved Oxygen Probe, β. At the gold cathode of the dissolved oxygen probe, the dissolved oxygen is cathodically reduced according to the faradaic reaction:

$$O_2 + 2H_2O + 4e^- = 4OH^-$$

at a rate given by

$$I = -4AFD^{V}_{O_2}\left[\frac{dC^{V}_{O_2}}{dx}\right]_{x^s} = -4AFD^{V}_{O_2}a^{V}_{O_2}. \quad (14)$$

The current response, I_o, is therefore

$$I_o = \left[\frac{4AFC^{B}_{O_2}}{B_o}\right] \quad (15)$$

where

$$B_o = \left[\frac{\delta_{V}}{D^{V}_{O_2}} + \frac{\delta_{IV}}{D^{IV}_{O_2}} + \frac{\delta_{III}}{D^{III}_{O_2}} + \frac{\delta_{II}}{D^{II}_{O_2}} + \frac{\delta_{I}}{D^{I}_{O_2}}\right]. \quad (16)$$

It is a normal practice to calibrate the dissolved oxygen electrode by relating the current response to the oxygen concentration in the solution in contact with the gas-permeable membrane. This is usually carried out before overlaying the probe with any membranes or the biofilm. Under such calibration conditions, δ_I, δ_{II}, and δ_{III} are zero and Eq. 15 is reduced to

$$I = \beta C^{III}_{O_2} \quad (17)$$

where β is the characteristic constant of the dissolved oxygen probe and is given by

$$\beta = \frac{4AF}{\left[\frac{\delta_{V}}{D^{V}_{O_2}} + \frac{\delta_{IV}}{D^{IV}_{O_2}}\right]} \quad (18)$$

in which $C^{III}_{O_2}$ is the dissolved oxygen concentration of the solution in contact with the gas-permeable membrane, which in this case will be the concentration of the bulk solution. Since the diffusivity of oxygen in the electrolyte is normally much greater than that in the gas-permeable membrane, Eq. 18 becomes

$$\beta = \frac{4AFD^{IV}_{O_2}}{\delta_{IV}}. \quad (19)$$

The effect of temperature on the current response is the result of the effect of temperature on the diffusivity of the oxygen in the gas-permeable membrane IV. This can be described by the Arrhenius equation as shown in Eq. 20:

$$D^{oIV}_{O_2} = D^{IV}_{O_2}\exp\left[-\frac{E^{IV}_{O_2}}{RT}\right]. \quad (20)$$

The temperature effect on the current response is therefore given by

$$I = \beta^{o}\exp\left[-\frac{E^{IV}_{O_2}}{RT}\right]C^{III}_{O_2} \quad (21)$$

where

$$\beta^{o} = \left[\frac{4AFD^{oIV}_{O_2}}{\delta_{IV}}\right]. \quad (22)$$

In the presence of the membranes and biofilm, the current response, I_o in a buffer solution containing no biooxidizable organic, is given by substituting $C^{III}_{O_2}$ from Eq. 7:

$$I_o = \beta^{o}\exp\left[-\frac{E^{IV}_{O_2}}{RT}\right]\left[C^{B}_{O_2} + (\varphi_{O(I/III)}\delta_{III} + \varphi_{O(I/II)}\delta_{II} + \delta_{I})a^{I}_{o}\right]. \quad (23)$$

Buffer Solution Containing Biooxidizable Organic Substrate. In the membranes and the electrolyte, the general mass balance equation for both the bio-oxidizable substrate (A) and dissolved oxygen, the general solution and the boundary conditions are similar to those given by Eqs. 1–4 except that the concentration gradient in phase J is replaced by b^{J}_{o} for oxygen and b^{J}_{A} for the organic substrate. The mass balance for biofilm (II) will include the rate of biooxidation of the organic substrate as shown in Eq. 24.

$$D^{II}_{s}\frac{d^2C^{II}_{s}}{dx^2} - r_s = 0 \qquad [s = O_2; A]. \quad (24)$$

Only oxygen and not the biooxidizable organic, A, can diffuse through the gas-permeable membrane (IV) into the electrolyte. This implies that the concentration gradient of A at $x = x_{III}$ is zero or $b_A^{III} = 0$. On this basis, the concentration profiles for the two substrates in the various membranes (I, III, and IV), biofilm (II), and the electrolyte (V) are derived.

Liquid-Permeable Membrane (I) with Thickness = δ_I.

$$C_A^{I} = b_A^{I} x + C_A^{B} \tag{25}$$

$$C_{O_2}^{I} = b_o^{I} x + C_{O_2}^{B}. \tag{26}$$

Biofilm (II) with Thickness = δ_{II}. It is necessary to know the reaction rate equation for the bio-oxidation reaction occurring in the biofilm. Sensors are usually calibrated to operate within the substrate concentration range in which the sensor response is linearly related to the substrate concentration. Such a linear relationship is usually valid for dilute solutions and the reaction kinetics can usually be simplified. Assume a first-order reaction rate with respect to the bio-oxidizable organic concentration and that it is independent of the dissolved oxygen concentration. The enzymic oxidation of dopamine by polyphenolase (Palmer, 1963) satisfies these assumptions. The reaction rate for a biooxidation stoichiometry, $A + nO_2 =$ products, with first-order reaction kinetics with respect to A is

$$-\frac{r_{O_2}}{n} = -r_A = k_m E_o C_A \tag{27}$$

where k_m is the reactant constant and E_o is the active mass of the tissue. The concentration profile of A in the biofilm II given in Eq. 28 is derived by integrating Eq. 24 for substrate A with the relevant boundary conditions:

$$C_A^{II} = (C_A^{B} + b_A^{I}\delta_I)\left[\frac{\cosh\{m(\delta_{II} + \delta_I - x)\}}{\cosh(m\delta_{II})}\right] \tag{28}$$

where

$$m = \sqrt{\frac{k_m E_o}{D_A^{II}}}. \tag{29}$$

The concentration gradient of the substrate A in liquid membrane I is given by

$$b_A^{I} = -C_A^{B}\left[\frac{m\varphi_{A(II/I)}\tanh(m\delta_{II})}{1 + m\delta_I\varphi_{A(II/I)}\tanh(m\delta_{II})}\right]. \tag{30}$$

The dissolved oxygen concentration profile in the biofilm was similarly derived and is shown in Eq. 31.

$$C_{O_2}^{II} = \left[\frac{\cosh\{m(\delta_{II} + \delta_I - x)\}}{\cosh(m\delta_{II})} - 1\right] n\varphi_{AO(II)}[C_A^{B} + b_A^{I}\delta_I] + \varphi_{O(III/II)}b_o^{III}(x - \delta_I) + b_o^{I}\delta_I + C_{O_2}^{B} \tag{31}$$

where

$$\varphi_{AO(J)} = \frac{D_A^{J}}{D_{O_2}^{J}}.$$

Liquid-Permeable Membrane (III) with Thickness = δ_{III}. At the gas-liquid membranes interface, x_{III}, the concentration gradient of A is zero since no A passes through the interface. The steady-state concentration of A is therefore constant across the whole membrane. Oxygen passes through the interface and its concentration profile is given in Eq. 32 by solving Eq. 1 with the appropriate boundary conditions given by Eqs. 3, 4, and 8.

$$C_{O_2}^{III} = C_{O_2}^{B} + b_o^{I}\delta_I + b_o^{III}(x - \delta_I - \delta_{II}) + \varphi_{O(I/II)}b_o^{I}\delta_{II} + n\varphi_{AO(II)}[C_A^{B} + b_A^{I}\delta_I][m\delta_{II}\tanh(m\delta_{II}) + \operatorname{sech}(m\delta_{II}) - 1] \tag{32}$$

where the constant concentration gradient is

$$b_o^{III} = \varphi_{O(I/III)}b_o^{I} + [nm\varphi_{AO(II)}\varphi_{O(II/III)} \times \tanh(m\delta_{II})][C_A^{B} + b_A^{I}\delta_I]. \tag{33}$$

Gas-Permeable Membrane (IV) with Thickness = δ_{IV}. Only oxygen diffuses through this membrane into the electrolyte V of the dissolved oxygen probe. At its interface with the liquid-permeable membrane III and with the electrolyte V, gas-liquid phase equilibrium for oxygen is assumed and is described by Henry's law for dilute solution. The oxygen partial pressure profile in this membrane is thus derived and given by Eq. 34:

$$P_{O_2}^{IV} = H_{O_2}\left[C_{O_2}^{B} + b_o^{I}\delta_I + \varphi_{O(I/II)}b_o^{I}\delta_{II} + b_o^{III}\delta_{III} + b_o^{IV}(x - \delta_{III} - \delta_{II} - \delta_I)\right] + H_{O_2}n\varphi_{AO(II)}[C_A^{B} + b_A^{I}\delta_I] \times [m\delta_{II}\tanh(m\delta_{II}) + \operatorname{sech}(m\delta_{II}) - 1] \tag{34}$$

where

$$b_o^{IV} = \varphi_{O(III/IV)}b_o^{III}. \tag{35}$$

Electrolyte (V) with Thickness = δ_V. The dissolved oxygen concentration at the electrode surface is zero under limiting current conditions. The oxygen concentration profile in the electrolyte is therefore described by

$$C_{O_2}^{V} = C_{O_2}^{B} + b_o^{I}(\delta_I + \varphi_{O(I/II)}\delta_{II}) + b_o^{III}\delta_{III} + b_o^{IV}\delta_{IV} + b_o^{V}(x - \delta_{IV} - \delta_{III} - \delta_{II} + \delta_I) + n\varphi_{AO(II)}[C_A^{B} + b_A^{I}\delta_I] \times [m\delta_{II}\tanh(m\delta_{II}) + \operatorname{sech}(m\delta_{II}) - 1], \tag{36}$$

while the oxygen concentration gradient is given by

$$b_o^{V} = \varphi_{O(IV/V)}b_o^{IV}. \tag{37}$$

Since the oxygen concentration at the surface of the gold cathode is zero under limiting current conditions, Eq. 36 at $x = x_V$ ($= \delta_I + \delta_{II} + \delta_{III} + \delta_{IV} + \delta_V$) is zero. Combined with the concentration gradient relationships, the oxygen concentration gradient in the liquid-permeable membrane I can be derived and is shown in Eq. 38:

$$b_o^I = -\left[\frac{C_{O_2}^B}{D_{O_2}^I B_o}\right] - \frac{n\varphi_{AO(II)}}{D_{O_2}^I B_o}[C_A^B + b_A^I \delta_I] \times \left[\varphi_{O(II/I)}\left(B_o - \frac{\delta_I}{D_{O_2}^I}\right) m \tanh(m\delta_{II}) + \operatorname{sech}(m\delta_{II}) - 1\right]. \quad (38)$$

Sensor response to the concentration of biooxidizable substrate

The steady-state sensor response is usually taken as the difference between the steady-state current response in the air-saturated solution without the biooxidizable solute (I_o) and with the biooxidizable solute (I_s). Equation 23 gives I_o and I_s is obtained by solving Eqs. 17 and 32.

$$I_s = \beta\left[C_{O_2}^B + b_o^I(\delta_I + \varphi_{O(I/II)}\delta_{II}) + b_o^{III}\delta_{III}\right] + \beta(C_A^B + b_A^I\delta_I)n\varphi_{AO(II)}[m\delta_{II}\tanh(m\delta_{II}) + \operatorname{sech}(m\delta_{II}) - 1]. \quad (39)$$

The functional equation for the sensor response, $[I_o - I_s]$, is then given by Eq. 40 in terms of the oxygen concentration gradients in liquid-permeable membrane I prior to and after the addition of the biooxidizable solute.

$$(I_o - I_s) = \beta[\varphi_{O(I/III)}\delta_{III} + \varphi_{O(I/II)}\delta_{II} + \delta_I][a_o^I - b_o^I] + \beta[C_A^B + b_A^I\delta_I]n\varphi_{AO(II)}[1 - \operatorname{sech}(m\delta_{II}) - m\{\delta_{II} + \varphi_{O(II/III)}\delta_{III}\}\tanh(m\delta_{II})] \quad (40)$$

where a_o^I, b_o^I, and b_A^I are given by Eqs. 12, 38, and 30, respectively. In the case where $m\delta_{II}$ is large or $\tanh(m\delta_{II}) \to 1$ and $\operatorname{sech}(m\delta_{II}) \to 0$, then

$$(I_o - I_s) = \beta[\varphi_{O(I/III)}\delta_{III} + \varphi_{O(I/II)}\delta_{II} + \delta_I][a_o^I - b_o^I] + \beta[C_A^B + b_A^I\delta_I]n\varphi_{AO(II)}[1 - m\{\delta_{II} + \varphi_{O(II/III)}\delta_{III}\}] \quad (41)$$

$$[a_o^I - b_o^I] = \frac{n\varphi_{AO(II)}\varphi_{O(II/I)}}{B_o\delta_{II}}\left[m\delta_{II}\left(B_o - \frac{\delta_I}{D_{O_2}^I}\right) - \frac{\delta_{II}}{D_{O_2}^{II}}\right] \times [C_A^B + b_A^I\delta_I] \quad (42)$$

and

$$b_A^I = -C_A^B\left[\frac{m\varphi_{A(II/I)}}{1 + m\delta_I\varphi_{A(II/I)}}\right]. \quad (43)$$

However, experimental observations showed that $\delta_I/D_{O_2}^I \ll B_o$ and $m\delta_{II} \gg \delta_{II}/(B_o D_{O_2}^{II})$. The functional relationship for the sensor response is therefore reduced to

$$[I_o - I_s] = \beta n\left[\frac{\varphi_{AO(II)} + \varphi_{AO(I)}\varphi_{KD}}{1 + \varphi_{KD}}\right]C_A^B \quad (44)$$

where the kinetic-diffusion parameter, φ_{KD}, is given by

$$\varphi_{KD} = m\delta_I\varphi_{A(II/I)} = \frac{m\delta_{II}}{\{k_{LA(I)}/k_{LA(II)}\}} \quad (45)$$

in which $m\delta_{II}$ is the bioactive material loading factor, similar to the enzyme loading factor proposed by Olsson et al. (1986) for their enzymatic sensor. $k_{LA(I)}$ [$= (D_A/\delta)_I$] and $k_{LA(II)}$ [$= (D_A/\delta)_{II}$] are the mass-transfer coefficients for A in the liquid-permeable membrane I and in the biofilm II, respectively. The effect of temperature on the various diffusion and kinetic-diffusion parameters are given by the Arrhenius equation.

$$\varphi_{AO(J)} = \varphi_{AO(J)}^o \exp\left[-\frac{E_{AO(J)}}{RT}\right] \quad (46)$$

where $\varphi_{AO(J)}^o$, $E_{AO(J)}$ are, respectively, the frequency factor and the difference in the activation energies associated with the diffusion of biooxidizable component A (E_A) and oxygen (E_{O_2}) in the membrane J. Similarly the temperature effect on the kinetic-diffusion parameter, φ_{KD}, is given by

$$\varphi_{KD} = \varphi_{KD}^o \exp\left[-\frac{E_{KD}}{RT}\right] \quad (47)$$

where

$$E_{KD} = \frac{E_K + E_{A(II)} - 2E_{A(I)}}{2} \quad (48)$$

in which E_K, $E_{A(I)}$, and $E_{A(II)}$ are the activation energies associated with the biooxidation reaction and the diffusion of A in membranes I and II, respectively.

Phenomenological parameters

Equation 44 shows that the current response varies directly with the solute concentration. The sensor sensitivity given by Eq. 49 intrinsically depends on the sensitivity (β) of the dissolved oxygen probe and the stoichiometric factor (n) of the biooxidation reaction:

$$S = \frac{d[I_o - I_s]}{dC_A^B} = \beta n\left[\frac{\varphi_{AO(II)} + \varphi_{AO(I)}\varphi_{KD}}{1 + \varphi_{KD}}\right]. \quad (49)$$

It also depends on the bioactive material loading factor and the diffusion characteristics of the liquid-permeable membrane (I) and the biofilm (II) with respect to the two reactants. The design of a highly sensitive biosensor therefore requires proper selection of the liquid-permeable membrane

and the immobilization technique such that the ratio of the diffusivity of the biooxidizable solute A to that of oxygen is high in both the liquid-permeable membrane and the biofilm. Since the organic solute is generally heavier and has larger molecular size than oxygen, $\varphi_{AO(I)}$ and $\varphi_{AO(II)}$ would be expected to be less than 1.0. At a ratio of 1, the sensitivity is equal to βn. This suggests that for a stoichiometric factor of 1, the sensitivity of the biosensor would always be lower than that of the dissolved oxygen probe.

Assuming that the mass of immobilized bioactive material does not affect the diffusivities of the solutes and since the parameter, m, given by Eq. 29 is a function of the mass of the immobilized bioactive material, then differentiating Eq. 49 with respect to m gives

$$\frac{dS}{dm} = \beta n \left[\frac{\varphi_{A(II/I)} \delta_I [\varphi_{AO(I)} - \varphi_{AO(II)}]}{[1 + \varphi_{KD}]^2} \right]. \tag{50}$$

The manner by which the bioactive material loading factor (m), or indirectly the amount of immobilized material in the biofilm, affects the sensor sensitivity depends on the relative diffusivity of A to that of oxygen in the liquid-permeable membrane and in the biofilm such that

$$\frac{dS}{dm} \gtreqless 0 \quad \text{if} \quad \varphi_{AO(I)} \gtreqless \varphi_{AO(II)}. \tag{51}$$

Experimental

The model was verified using experimental data obtained with a recently developed apple-tissue dopamine sensor (Tan and Chen, 1993) at different temperatures, pHs, and using biofilm immobilized with different masses of apple fines. The sensing mechanism is based on the enzymic oxidation of dopamine by the polyphenolase in the apple tissues. The stoichiometric ratio, n, for the reaction is 1. Two sets of experiments were carried out. The unmodified dissolved oxygen probe was first calibrated against known concentrations of dissolved oxygen at different temperatures. The sensor response/concentration/temperature sets of data were regressed according to Eq. 21. Experimental data were also obtained using the apple-tissue dopamine sensor at different temperatures and pHs of the solution and with different masses of immobilized apple fines in the biofilm. These results were used to verify the model by correlating the data according to Eqs. 44, 46 and 47.

Fabrication of the apple-tissue dopamine sensor

Apple slides were crushed and pulverized. The fines were repeatedly washed and centrifuged to remove the esters and sugars in the tissues. This pretreatment step was found necessary to improve the accessibility of the polyphenolase in the tissue for the bio-oxidation process (Tan and Chen, 1993). The fines were dried under vacuum at room temperature. A known weight of the dry apple fines were mixed with 10^{-7} m^3 of 40 kg/m^3 polyvinyl alcohol into a smooth paste and then applied evenly over a polycarbonate membrane. This was left to dry in air and then stored in the refrigerator at 277 K in a covered petri dish. The dopamine sensor was prepared by placing the biofilm with its polycarbonate membrane backing on top of the Teflon gas membrane of a YSI 50 dissolved oxygen probe such that the biofilm faced outwards. The biofilm was covered with another similar polycarbonate membrane to prevent any dislodged apple fines from contaminating the test solution during measurements. The polycarbonate membrane sandwiched biofilm was stretched and wrapped tightly over the Teflon gas-membrane and properly secured with a tightly fitting rubber O-ring.

Experimental procedure

Calibration of the Dissolved Oxygen Probe. The YSI 50 dissolved oxygen probe was calibrated to relate the sensor current to the dissolved oxygen concentration in a solution at different pHs and temperatures. The probe was immersed in a buffer solution maintained at a constant temperature by passing water from a constant-temperature bath through the jacket of the container. Air/nitrogen mixture was continuously bubbled through the solution to minimize diffusion effects in the solution. The dissolved oxygen concentration given by the probe meter was noted when the reading remained steady. The electrodes were then connected to a potentiostat adjusted to give a constant cell voltage of -0.8 V across the gold cathode and the silver anode. The steady-state current, corresponding to the oxygen concentration given by the probe meter, was noted. The experiment was repeated for different oxygen concentrations by altering the air/nitrogen ratio, pH, or the temperature of the solution.

Response of the Apple Tissue Dopamine Sensor. The tissue sensor was immersed in a phosphate buffer of known pH, then constantly agitated by a magnetic stirrer and also by a continuous stream of air from a compressed air cylinder. The solution was kept at a constant temperature by passing constant-temperature water through the water jacket of the container. A potentiostat provided a constant cell voltage of -0.8 V across the gold cathode and silver anode of the dissolved oxygen probe. The sensor current was monitored on a strip chart recorder and also simultaneously displayed on a HP 3466A digital multimeter. When the system reached steady-state conditions, the current (I_o) was noted. A known amount of a freshly prepared dopamine solution was introduced into the buffer and the system was left to equilibrate. The steady-state current (I_s) was noted. The experiment was repeated for other dopamine concentrations, pHs, temperatures, and different amounts of apple fines immobilized in the biofilm.

Results and Discussions

Calibration of the dissolved oxygen probe

The current-concentration data obtained using the unmodified dissolved oxygen probe at various temperatures were correlated according to Eq. 21 by the nonlinear regression technique. The resulting correlation is given by

$$I = 10.28 \exp\left[-\frac{30{,}592}{RT} \right] C^B_{O_2} \tag{52}$$

where I is in A and $C^B_{O_2}$ is in mol/m^3. The correlation incurred a mean fractional error of 0.0064 with a standard de-

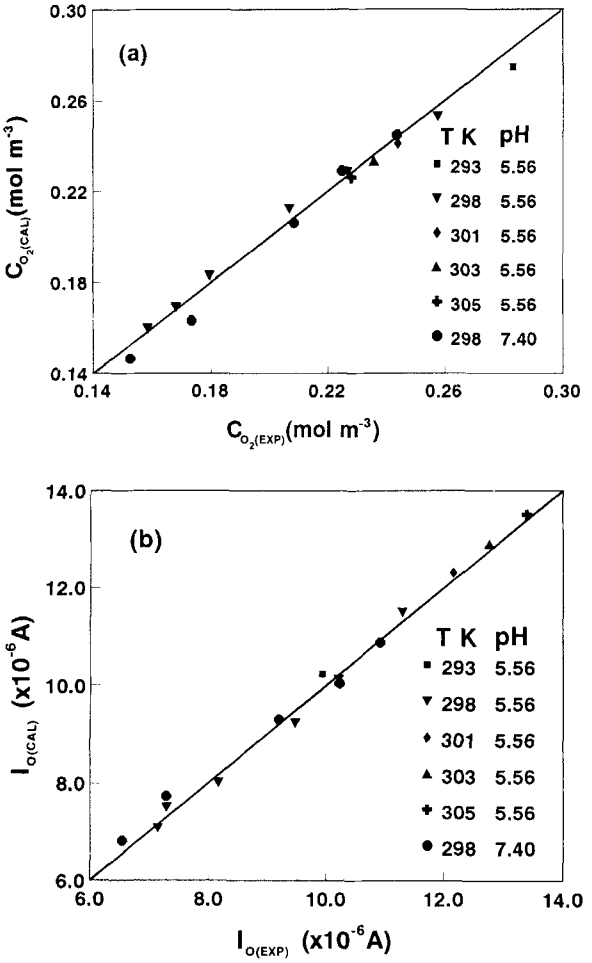

Figure 3. Experimental values vs. corresponding values calculated from the correlation for the dissolved oxygen probe according to the derived model.

(a) Oxygen concentration. (b) Current response.

viation of 0.022 based on oxygen concentration (Figure 3a) and a mean fractional error of 0.0069 with a standard deviation of 0.023 with respect to current response (Figure 3b). The corresponding mean absolute fractional errors are 0.0187, with a standard deviation of 0.0140 for the concentration and 0.019, with a standard deviation of 0.0148 for the current response. The fractional error was calculated as a ratio of (calculated value−experimental value) to the experimental value. These results show that the model adequately describes the operational characteristics of the dissolved oxygen probe. It was found that pH of the solution affects only the oxygen saturation concentration in the solution and has little or no effect on the diffusivity of the solute.

The sensitivity of the probe given by β ranges from 3.32×10^{-5} to 5.92×10^{-5} A·m^3/mol or 1.038–1.851 μA/ppm over the temperature range 291–305 K. Hale and Hitchman (1980) reported a sensitivity range of 2.7 to 1.2 μA/ppm with electrolyte thickness range of 3.5×10^{-6} to 2.35×10^{-4} m at 296 K compared with 1.283 μA/ppm (4.1×10^{-5} A·m^3/mol) for the present study with YSI 50 dissolved oxygen probe. The difference in the sensitivity may be attributed to the different thickness of the Teflon membrane used in the two cases: 3×10^{-5} m in the present study compared with the 1.25×10^{-5} m used by Hale and Hitchman (1980). At 296 K, $\beta=4.1\times10^{-5}$ A·m^3/mol, and with a cathodic area of 3.246×10^{-5} m^2, the diffusivity of oxygen in the 3×10^{-5}-m-thick Teflon membrane of the present probe is given by Eq. 19 as 9.83×10^{-11} m^2/s compared with the graphical value of 8.71×10^{-11} m^2/s and calculated value of 8.20×10^{-11} m^2/s reported by Hale and Hitchman (1980).

Sensing characteristics of the tissue dopamine sensor

The sensing characteristics of the apple-tissue dopamine sensor was studied over a temperature range of 288–308 K at constant pH of 5.56 with a total of 68 sets of data and over a pH range of 4.89 to 8.49 at a constant temperature of 298 K with a total of 60 sets of data. Both of these sets of experiment were carried out with the same biofilm containing 3.02×10^{-5} kg of pretreated apple fines with a film thickness of 3×10^{-4} m. Experiments were also carried out using biofilms containing 2.01×10^{-5} kg ($\delta_{II}=6.33\times10^{-4}$ m) and 1.55×10^{-5} kg ($\delta_{II}=3.5\times10^{-4}$ m) of immobilized apple fines. It was not possible to control the thickness of the biofilm; however, the film thickness only affected the bulk porosity of the film and not the pore characteristics within the apple-tissue structure. Since the polyphenolase is in the tissue structure, the pore diffusion resistance in the tissue accounts for most of the diffusion resistance in the biofilm. As such it would be justifiable to assume that the mass of immobilized apple fines and in particular the film thickness would have little or no effect on the effective diffusivity of the solute in the biofilm.

The effects of the temperature, pH, and mass of the immobilized apple fines in the biofilm on the sensor response, (I_o-I_s), to dopamine in an air-saturated phosphate buffer solution are shown in Figures 4 and 5. A linear sensor response–concentration relationship was obtained up to about 0.2 mol/m^3 of dopamine. Sensitivity increased with temperature and was not significantly affected by the solution pH or the mass of immobilized apple fines in the biofilm.

Verification of the model

The model was verified using the 68 data sets obtained with the same biofilm containing 3.02×10^{-5} kg of apple fines, pH 5.56, and for different temperatures. These data were regressed according to Eq. 44 with the various diffusion and kinetic-diffusion constants substituted by the Arrhenius expressions given in Eqs. 46 and 47. The Arrhenius expression for the sensitivity of the dissolved oxygen probe or β given in Eq. 52 is incorporated into Eq. 44 for the regression. The resulting equation obtained is shown in Eq. 53:

$$[I_o-I_s]=10.28\exp\left[-\frac{30{,}592}{RT}\right]\times\left(\frac{0.0205\exp\left[\frac{8{,}670}{RT}\right]+10.26\exp\left[-\frac{8{,}020}{RT}\right]}{1+0.994\exp\frac{-342.3}{RT}}\right)C_A^{\beta}. \quad (53)$$

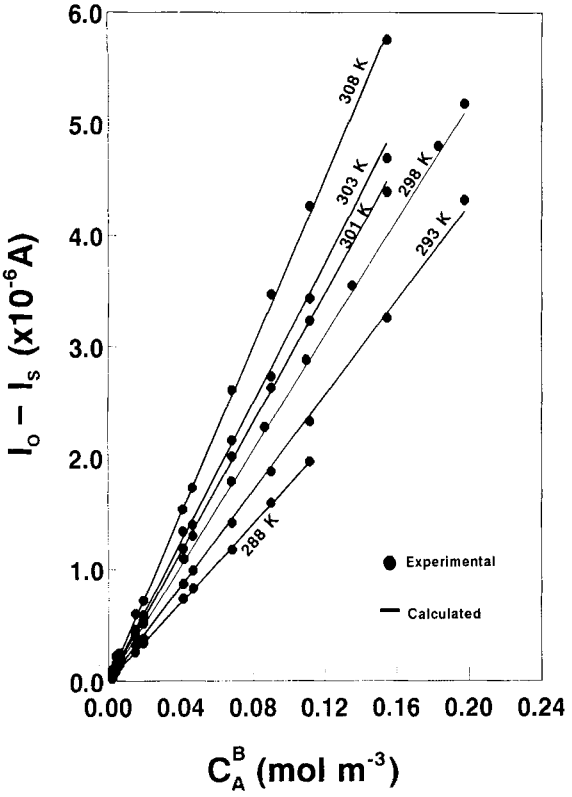

Figure 4. Temperature effect on the sensor response to dopamine concentration at pH 5.56.

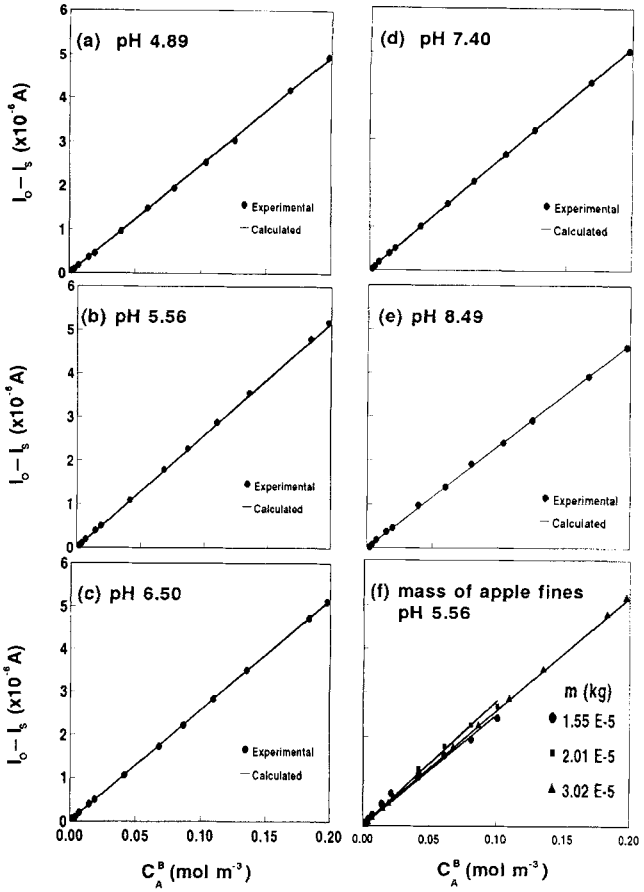

Figure 5. Sensor response to dopamine concentration at 298 K and different pHs for biofilm containing 3.02×10^{-5} kg of immobilized apple fines (a)–(e) and at pH 5.56 for biofilm containing different masses of immobilized apple fines (f).

The correlation incurred a mean fractional error of 0.0122 with a standard deviation of 0.129. The corresponding mean absolute fractional error was 0.0609 with a standard deviation of 0.114. The solid lines in Figure 4 were computed from the regressed Eq. 53 and compared with the experimental data plotted as symbols in the same figure. These results show conclusively that the proposed model describes adequately the sensing mechanism and characteristics of the dopamine biosensor.

The functional relationships of the three biosensor parameters, $\varphi_{AO(I)}$, $\varphi_{AO(II)}$, and φ_{KD}, are given in Eqs. 54, 55 and 56, respectively:

$$\varphi_{AO(I)} = \frac{D_A^I}{D_{O_2}^I} = 10.32 \exp\left[-\frac{7{,}678}{RT}\right] \tag{54}$$

$$\varphi_{AO(II)} = \frac{D_A^{II}}{D_{O_2}^{II}} = 0.0205 \exp\left[\frac{8{,}670}{RT}\right] \tag{55}$$

$$\varphi_{KD} = \left[\frac{m\delta_{II}}{\left(\frac{k_{LA(I)}}{k_{LA(II)}}\right)}\right] = 0.994 \exp\left[-\frac{342.3}{RT}\right]. \tag{56}$$

Figure 6 shows that with increasing temperature, the diffusivity ratio of dopamine to oxygen in the polycarbonate membrane increases while that in the biofilm decreases. In all cases, however, the diffusivity ratio is always less than 1 (about 0.42–0.51 in the polycarbonate membrane and 0.77–0.61 in the biofilm for 288–308 K). This is consistent with the relative molecular weight and size of dopamine and oxygen. The effect of temperature on the kinetic-diffusion parameter is small (0.86–0.87 for the same temperature range).

Equations 54–56 show that the relative magnitude of the activation energies associated with the diffusion of dopamine and oxygen in the polycarbonate membrane and in the biofilm and that associated with the enzymatic oxidation of dopamine in the biofilm are

$$E_{A(I)} > E_{O_2(I)}, \quad E_{A(II)} < E_{O_2(II)}, \quad \text{and} \quad E_k > 2E_{A(I)} - E_{A(II)}.$$

The effect of temperature on the diffusion of dopamine and oxygen in the polycarbonate membrane (I) is consistent since the diffusion of dopamine is accompanied with a higher activation energy than that for oxygen, as would be expected for the difference in the molecular weight and size of the two solutes. However, the anomalous diffusion phenomena observed in the biofilm (II) can be attributed to the single-site reaction mechanism for the enzymic oxidation of dopamine

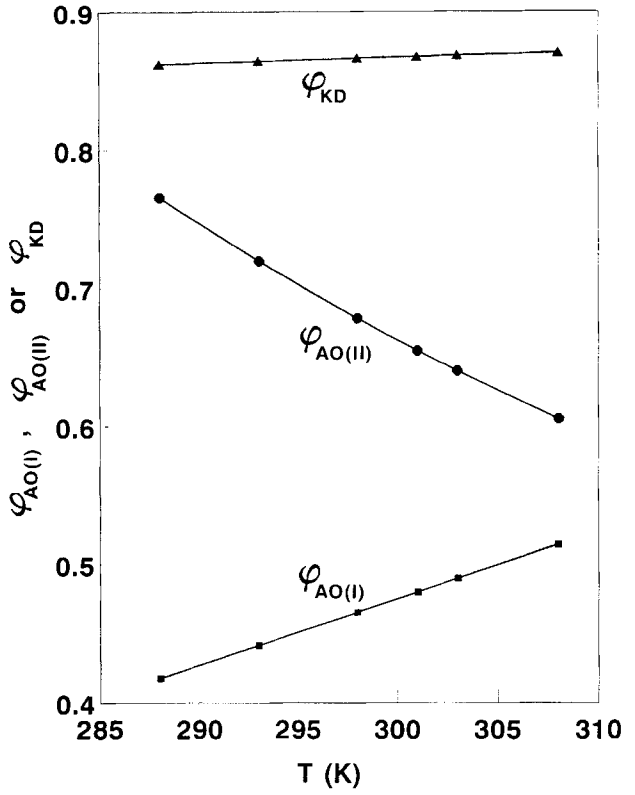

Figure 6. Temperature effect on the kinetic-diffusion parameter and ratios of the effective diffusivity of dopamine to oxygen in the polycarbonate membrane and in the biofilm.

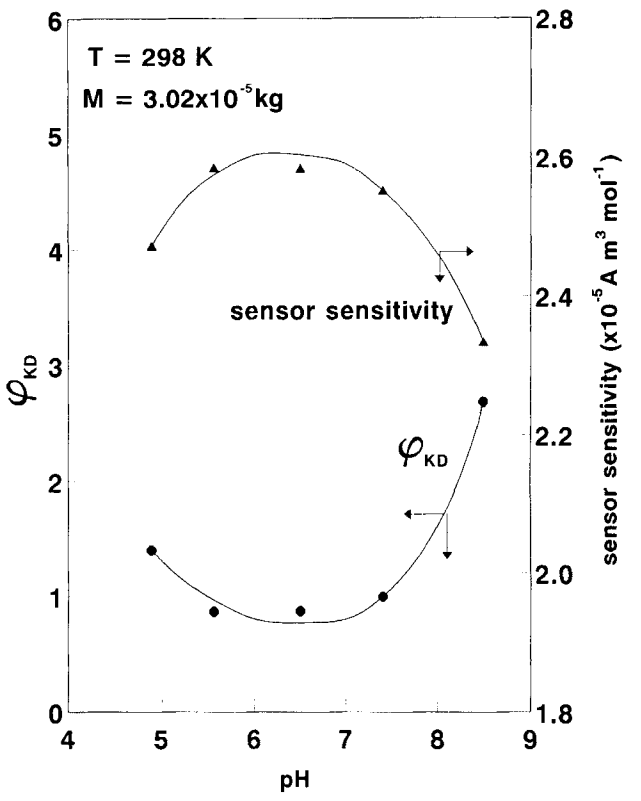

Figure 7. pH effect on the kinetic-diffusion parameter and sensor sensitivity.

(Tan and Chen, 1992). The diffusivity term for oxygen in the biofilm would necessarily incorporate the effect of the oxygen adsorption on the active sites. The combined diffusion/adsorption phenomena would account for the larger activation energy than that for the diffusion of the dopamine in the biofilm. Under the present conditions of excess oxygen and low dopamine concentration, the reaction kinetics is first order in dopamine (Tan and Chen, 1992) and it is most unlikely that the anomalous diffusion phenomena in the biofilm arises from this simplification. The small temperature effect on the kinetic-diffusion parameter, φ_{KD}, may be attributed to the effect of temperature on the kinetic constant and the diffusion coefficient of dopamine in the biofilm being compensated by the opposing effect of temperature on the diffusion of dopamine in the polycarbonate membrane. It can be shown that the equation for the sensitivity of the dopamine tissue sensor given by Eq. 49 with appropriate substitution of the parameters given by Eqs. 52 and 54–56 is a monotonically increasing function with respect to temperature, that is, the sensitivity increases with increasing temperature within the normal working temperature for biosensors. There is no optimum operating temperature for maximum sensitivity except for the limitation of thermal deactivation of the enzyme.

Model and the effect of pH

The data obtained at 298 K with the same biofilm containing 3.02×10^{-5} kg of immobilized apple fines at different pHs were similarly correlated by the model on the assumptions that pH affects only the enzyme activity and hence the reaction constant of the biooxidation reaction and has little or no effect on the diffusivity of the solutes. The data for each pH was regressed to evaluate φ_{KD} with $\beta = 4.46\times10^{-5}$ A·m^3/mol from Eq. 52, $\varphi_{AO(I)} = 0.4654$ from Eq. 54 and $\varphi_{AO(II)} = 0.6780$ from Eq. 55. Figure 7 shows the effect of pH on the kinetic-diffusion parameter, φ_{KD}, or the effective reaction constant ($k_m E_o$), since pH has little or no effect on the diffusivities. The effective reaction constant approached a minimum at about pH = 6 while increasing sharply at pH = 4.89 and 8.49. Harel et al. (1965) and Walker and Hulme (1966) reported that the enzymic activity of phenolase complex in apple tissues is optimum at two different pHs (5.1 and 7.3) in phosphate buffer, depending on the fraction from which the enzyme is extracted. The extract from the mitochondrial fraction will show both optima, whereas that from the chloroplast fraction would show only the optimum at 5.1. In the present study, no deliberate effort was made to isolate these fractions, and hence the possibility of the apple fines, to show that two optima pH conditions are likely. The deviation in the optima values reported can be attributed to the interaction effect due to the mass transfer and adsorption phenomena. Figure 7 also shows that the sensor sensitivity reached an optimum at about pH 6, at which the kinetic-diffusion parameter is also a minimum. As shown in Eq. 51, the manner by which the kinetic-diffusion parameter affects the sensor sensitivity depends on the relative values of $\varphi_{AO(I)}$ and $\varphi_{AO(II)}$. In this study, $\varphi_{AO(I)} < \varphi_{AO(II)}$ up to a temperature of 316 K,

which would therefore explain the maximum sensitivity at about pH 6 in Figure 7.

Figures 5a–5e show the experimental points plotted against the solid line computed from the correlation. For a total of 60 data points, the correlation showed a mean fractional error of −0.0286 with a standard deviation of 0.243. The corresponding mean absolute fractional error is 0.0702, with a standard deviation of 0.2345. The good correlation results justify the assumption that pH has little or no effect on the diffusivities of the solutes and also confirmed the adequacy of the model in describing the sensing characteristics of the dopamine tissue sensor.

Effect of mass of immobilized apple fines in the biofilm

Although the apple fines used were from the same batch of preparation, it was not possible to prepare biofilms with thickness proportional to the mass used. However, the experimental results suggested that the diffusion phenomena in the biofilm were most probably associated with the diffusion of the solutes into the tissue structure, including oxygen adsorption on the active sites. Hence, the film porosity, which depends on the packing of the particles in the film and the film thickness, may have little or no effect on $\varphi_{AO(II)}$. On this basis, the 30 data points obtained using the three biofilms in which different amounts of apple fines were immobilized at 298 K and pH 5.56 were correlated with $\beta = 4.46 \times 10^{-5}$ A·m^3/mol, $\varphi_{AO(I)} = 0.4654$, and $\varphi_{AO(II)} = 0.6780$. The regressed values of φ_{KD} for the three biofilms are 1.3394 (1.55×10^{-5} kg, 3.5×10^{-4} m thick); 0.3212 (2.01×10^{-5} kg, 6.33×10^{-4} m thick); and 0.8659 (3.02×10^{-5} kg, 3.0×10^{-4} m thick). Figure 5f shows the experimental points (as symbols) with the solid lines computed from the correlations. The correlation incurred a mean fractional error of 0.0895 with a standard deviation of 0.113. The corresponding mean absolute fractional error is 0.0991, with a standard deviation of 0.105. Although the error is higher than the other correlations, it is within reasonable limits to suggest that the resistance due to the diffusion in the tissue structure and interacting adsorption phenomena predominate over that due to the interparticle diffusion in the biofilm. Due to the difference in the enzymatic activity of the polyphenolase in the different parts of apple (Harel et al., 1965; Walker and Hulme, 1966), the apple fines were inhomogeneous. Therefore, just like many other sensors, it is necessary to calibrate the sensor for every new biofilm installed.

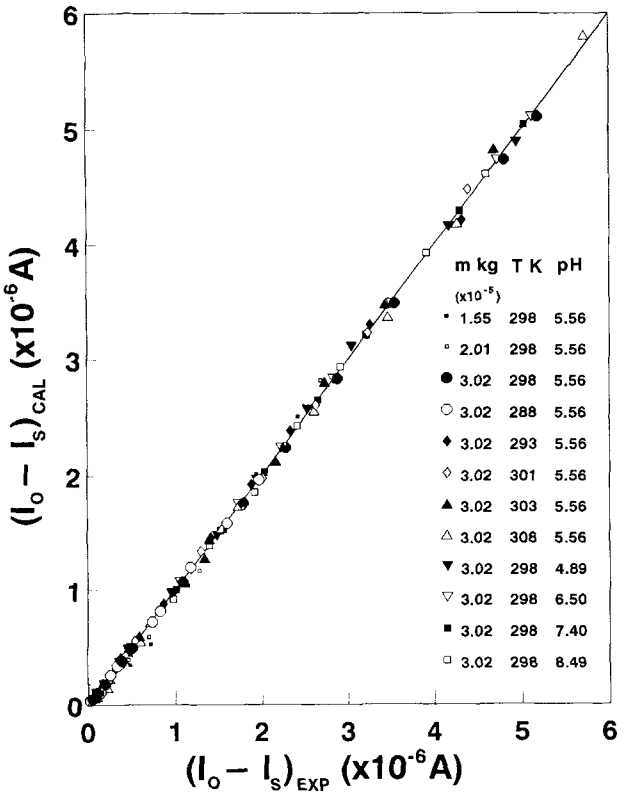

Figure 8. Experimental sensor response vs. calculated values from the model.

Overall assessment of the model

Figure 8 shows the plot of all the 134 experimental data points against the corresponding values calculated from the correlations. The overall mean fractional error for all 134 data points is 0.0097, with a standard deviation of 0.199, whereas the overall mean absolute fraction error is 0.0801, with a standard deviation of 0.183. These results show that the proposed model adequately describes the effect of the various rate phenomena on the sensing characteristics of the dopamine apple-fines sensor.

Conclusions

A mathematical model was developed to describe the steady-state sensing characteristics of a bio-oxidation-related biosensor, taking into consideration the various rate processes involved in the sensing process. The sensitivity of the biosensor depended intrinsically on the dissolved oxygen probe sensitivity and directly on the stoichiometric ratio of oxygen to solute in the biocatalyzed oxidation process. It also depended on the diffusion characteristics of the two reactants in the liquid-permeable membrane and in the biofilm coupled with the bioactive material loading factor of the biofilm. Using an apple tissue dopamine sensor, there was a good correlation of the sensor response at different temperatures, pHs, and different amounts of immobilized apple fines in the biofilm according to the proposed model. The resulting correlation showed an overall mean fractional error of 0.0097, with a standard deviation of 0.199, and an overall mean absolute fractional error of 0.0801, with a standard deviation of 0.183. The model also described equally well the sensing characteristics of the YSI 50 dissolved oxygen probe, with a mean absolute fractional error of 0.019, and a standard deviation of 0.015, with respect to its current response for a given oxygen concentration in the solution. The model showed that obtaining a highly sensitive biosensor depends significantly on the correct choice of liquid-permeable membrane, and on the immobilization technique to achieve a high ratio of the effective diffusivity of the solute relative to that of oxygen in both the liquid-permeable membrane and the biofilm. Increases in the kinetic-diffusion parameter, which contains the effective reaction constant of the biooxidation

process, will enhance the sensor sensitivity if the relative diffusivity of the solute to oxygen in the liquid-permeable membrane is higher than that in the biofilm, and vice versa. The reaction constant will have no effect on the sensitivity if both the membrane and biofilm give the same relative diffusivity of the two reactants.

Acknowledgments

The authors gratefully acknowledge the financial support for the sensor project and the award of a research scholarship to Y. Chen by the National University of Singapore.

Notation

A = electrode area (m^2)
a_1 = constant in Eq. 2 ($mol \cdot m^{-3}$)
B_o = total mass-transfer resistance as defined by Eq. 16 ($s \cdot m^{-1}$)
F = Faraday constant ($A \cdot s \cdot mol^{-1}$)
H = Henry's law constant ($Pa \cdot m^3 \cdot mol^{-1}$)
r = rate of reaction ($mol \cdot m^{-3} \cdot s^{-1}$)
R = gas constant (8.314 $J \cdot mol^{-1} \cdot K^{-1}$)
S = sensor sensitivity ($A \cdot m^3 \cdot mol^{-1}$)
T = temperature (K)

Superscript

o = denotes frequency factor in Arrhenius equation

Literature Cited

Albery, W. J., and D. H. Craston, "Amperometic Enzyme Electrodes: Theory and Experiment," *Biosensors Fundamentals and Applications*, A. P. Y. Turner, I. Karube, and G. S. Wilson, eds., Oxford Univ. Press, New York, p. 180 (1987).

Arnold, M. A., and G. A. Rechnitz, "Biosensors Based on Plant and Animal Tissue," *Biosensors Fundamentals and Applications*, A. P. Y. Turner, I. Karube, and G. S. Wilson, eds., Oxford Univ. Press, New York, p. 30 (1987).

Blaedl, W. J., T. R. Kissel, and R. C. Boguslaski, "Kinetic Behaviour of Enzymes Immobilized in Artificial Membranes," *Anal. Chem.*, **44**, 2030 (1972).

Brady, J. E., and P. W. Carr, "Theoretical Evaluation of the Steady-State Response of Potentiometric Enzyme Electrodes," *Anal. Chem.*, **52**, 977 (1980).

Clark, L. C., Jr., "The Enzyme Electrode," *Biosensors Fundamentals and Applications*, A. P. Y. Turner, I. Karube, and G. S. Wilson, eds., Oxford Univ. Press, New York, p. 3 (1987).

Eddowes, M. J., "Theoretical Methods for Analyzing Biosensor Performance," in *Biosensors: A Practical Approach*, A. E. G. Cass, ed., Oxford Univ. Press, New York, p. 211 (1990).

Firouztale, E., M. J. Skerpon, and J. S. Ultman, "A Spherical Model of the Clark Electrode in a Flowing Liquid Medium," *J. Electroanal. Chem.*, **134**, 1 (1982).

Gough, D. A., and J. K. Leypoldt, "A Novel Rotated Disc Electrode and Time Lag Method for Characterizing Mass Transport in Liquid Membrane System," *AIChE J.*, **26**, 1013 (1980).

Gough, D. A., J. Y. Lucisano, and P. H. S. Tse, "Two-Dimensional Enzyme Electrode Sensor for Glucose," *Anal. Chem.*, **57**, 2351 (1985).

Hale, J., and M. L. Hitchman, "Some Considerations of the Steady-State and Transient Behaviour of Membrane-Covered Dissolved Oxygen Detectors," *J. Electroanal. Chem.*, **107**, 281 (1980).

Hameka, H. F., and G. A. Rechnitz, "Theory of the Biocatalytic Membrane Electrode," *J. Phys. Chem.*, **87**, 1235 (1983).

Harel, E., A. M. Mayer, and Y. Shain, "Purification and Multiplicity of Catechol Oxidase from Apple Chloroplasts," *Phytochemistry*, **4**, 783 (1965).

Jensen, O. J., T. Jacobsen, and K. Thomsen, "Membrane-Covered Oxygen Electrodes I. Electrode Dimensions and Electrode Sensitivity," *J. Electroanal. Chem.*, **87**, 203 (1978).

Jochum, P., and B. R. Kowalski, "A Coupled Two-Compartment Model for Immobilized Enzyme Electrodes," *Anal. Chim. Acta*, **144**, 25 (1982).

Karube, I., "Macroorganism Based Sensors," *Biosensors Fundamentals and Applications*, A. P. Y. Turner, I. Karube, and G. S. Wilson, eds., Oxford Univ. Press, New York, Tokyo, p. 13 (1987).

Karube, I., "Microbial Sensors for Process and Environmental Control," in *Fundamentals and Application of Chemical Sensors*, D. Schuetzle and R. Hammerle, eds., ACS Symposium Ser., **309**, (1986).

Lemke, K., "Mathematical Simulation of an Amperometric Enzyme-Substrate Electrode with a pO_2 based Sensor, Part 1: Mathematical Model and Simulation of the pO_2 Based Sensor," *Med. Biol. Eng. Comput.*, **26**, 523 (1988a).

Lemke, K., "Mathematical Simulation of an Amperometric Enzyme-Substrate Electrode with a pO_2 Basic Sensor, Part 2: Mathematical Simulation of the Glucose Oxidase Glucose Electrode," *Med. Biol. Eng. Comput.*, **26**, 533 (1988b).

Leypoldt, J. K., and D. A. Gough, "Model of a Two-Substrate Enzyme Electrode for Glucose," *Anal. Chem.*, **56**, 2896 (1984).

Mell, L. D., and J. T. Maloy, "A Model for the Amperometric Enzyme Electrode Obtained through Digital Simulation and Applied to the Immobilized Glucose Oxidase System," *Anal. Chem.*, **47**, 299 (1975).

Myland, J. C., and K. B. Oldham, "Membrane-Covered Oxygen Sensors: An Exact Treatment of the Switch-on Transient," *J. Electrochem. Soc.*, **131**, 1815 (1984).

Olsson, B. O., H. Lundback, J. Gillis, S. Scheller, and J. Nentwig, "Theory and Application of Diffusion Limited Amperometric Enzymic Electrode Detection in Flow Injection Analysis of Glucose," *Anal. Chem.*, **58**, 1046 (1986).

Palmer, J. K., "Banana Polyphenoloxidase Preparation and Properties," *Plant Physiol.*, **38**, 508 (1963).

Rechnitz, G. A., "Membrane Electrode Probes for Biological Systems," *Science*, **190**, 234 (1975).

Rechnitz, G. A., "Bioselective Membrane Electrode Probes," *Science*, **214**, 287 (1981).

Riedel, K., U. Alexiev, B. Neumann, M. Kuehn, R. Rennebergand, and F. Scheller, "A Microbial Sensor for BOD," *Biosensors Applications in Medicine, Environmental Protection and Process Control*, R. D. Schmid and F. Scheller, eds., GBF Monograph 13, VCH, Weinheim (1989).

Sidwell, J. S., and G. A. Rechnitz, "Progress and Challenges for Biosensors using Plant Tissue Materials," *Biosensors*, **2**, 221 (1986).

Tan, T. C., F. Li, and K. G. Neoh, "Microbial Membrane-Modified Dissolved Oxygen Probe for Rapid Biochemical Oxygen Demand Measurement," *Sensors & Actuators B*, **8**, 167 (1992).

Tan, T. C., and Y. Chen, "Enzymic Oxidation of Dopamine by Polyphenol Oxidaze," *Int. J. Chem. Kinet.*, **24**, 1023 (1992).

Tan, T. C., and Y. Chen, "Sensing Characteristics of an Immobilized Apple Powder Enzyme Sensor," *Sensors & Actuators B*, **17**, 101 (1993).

Tatsuma, T., and T. Watanabe, "Model Analysis of Enzyme Monolayer and Bilayer-Modified Electrodes: The Steady State Response," *Anal. Chem.*, **64**, 625 (1992).

Vacek, V., V. Linek, and J. Sinkule, "Transient Diffusion of Oxygen through the Three Spherical Layers of the Clark Oxygen Sensor," *J. Electrochem. Soc.*, **133**, 540 (1986).

Walker, J. R. L., and A. C. Hulme, "Studies on the Enzymic Browning of Apples: III. Purification of Apple Phenolase," *Phytochemistry*, **5**, 259 (1966).

Manuscript received July 9, 1993, and revision received Mar. 22, 1994.